Supplemental file 1: Treatment Emergent Adverse Events (TEAEs)

TEAEs are summarised by Medical Dictionary for Regulatory Activities (MedDRA) system organ class and preferred term in Table 5. There were no reported SAEs.

SUPPLEMENTAL TABLE 1: Treatment Emergent Adverse Event (TEAEs)

System Organ Class[a]	Preferred Term[a]	Worst CTCAE Grade[b]	Related to IMP[c]	Participants % (n=3)
Injury, poisoning and procedural complications	Tooth fracture	1	No	33.33% (1)
Gastrointestinal disorders	Vomiting	1	No	33.33% (1)
Gastrointestinal disorders	Constipation	1	No	33.33% (1)
Gastrointestinal disorders	Abdominal Pain	2	No	33.33% (1)
Skin and Subcutaneous tissue disorders	Erythema	1	No	33.33% (1)
General disorders and administration site conditions	Localised Oedema	1	No	33.33% (1)

[a] MedDRA

[b] CTCAE (Common Terminology Criteria for Adverse Events) v5 Grade

[c]All TEAEs were assessed by Investigator as probably unrelated to IMP

Supplemental file 2: PSMA-PET SUVs, and normal tissue gamma camera assessments post-administration AB001

SUPPLEMENTAL TABLE 2: Normal tissue SUV_{mean} from patient PSMA-PET images.

Tissue	SUVmean		
	Patient ID01	Patient ID02	Patient ID03
Salivary glands	18.5	13	19.8
Kidneys	19.2	16.1	11.4
Liver	11.3	21.8	12.5
Spleen	12.6	6.1	13.7
Blood pool	0.7	0.6	1.1
Bone Marrow	1.3	0.9	0.7
Small intestine including contents	5.4	17.1	16.1
Urinary bladder including contents	6.2	2.3	2.3

SUPPLEMENTAL TABLE 3: Normal tissue visual assessments of planar gamma camera images performed post-administration of ^{212}Pb-labelled PSMA-targeting AB001. Images were scored Yes (Y) or No (N) if an uptake was clearly visible.

Tissue	Patient ID01	Patient ID02	Patient ID03
Salivary glands	N	N	N
Kidneys	Y	Y	Y
Liver	N	N	Y
Spleen	N	N	N
Blood pool	N	N	N
Bone marrow	N	N	N
Small bowel including contents	N	N	N
Urinary bladder including contents	N*	Y	Y

*Limited bladder filling due to incontinence

SUPPLEMENTAL TABLE 4: Normal tissue visual assessments of SPECT images performed post- administration of ^{212}Pb-labelled PSMA-targeting AB001. Images were scored Yes (Y) or No (N) if an uptake was clearly visible.

Tissue	Patient ID01	Patient ID02	Patient ID03
Salivary glands	N	N	N
Kidneys	Y	Y	Y
Liver	N	N	Y
Spleen	N	N	N
Blood pool	Y	N	Y
Bone marrow	N	N	N
Small bowel including contents	N	N	N
Urinary bladder including contents	N*	Y	N

*Limited bladder filling due to incontinence

Supplemental file 3: Data used in Figure 5

Figure 5 serves to give an indication of the likelihood of visualizing smaller volumes with ^{212}Pb when imaging with a Siemens Symbia Intevo Bold SPECT. This study used a microdose of 10 MBq, and thus visualizing small volumes with low activity concentrations was challenging. Importantly, there cannot be a direct translation of the phantom results to the patient images, as several other factors, such as uptake in surrounding tissues, blood background, movement, increased attenuation, and biology, influence visualization for patients. Still, phantom images give information on what we could see in an idealized situation, and that can give an indication of the visualization probabilities in patients.

The National Electrical Manufacturers Association (NEMA) International Electrical Commission (IEC) PET Body Phantom was used to calculate contrast. The phantom was filled on separate occasions, with either ^{224}Ra or ^{212}Pb. The main imageable emissions of ^{224}Ra are from ^{212}Pb and daughters, and therefore the results of ^{224}Ra are used here as ^{212}Pb. The phantom images were acquired on a Siemens Symbia SPECT/CT with a medium energy collimator and an energy window of 20% centered on 240 keV and 5% dual scatter windows. A noncircular orbit was used, with 60 views of 30 seconds and acquisition during steps. Both scatter correction and attenuation correction based on CT were applied. One exception is the acquisition with 2 kBq/mL. This was a 3-minute acquisition with 20 kBq/mL in the spheres, which when scaled to a 30-minute acquisition is equivalent to 2 kBq/mL. The images were reconstructed with 30 iterations and 2 subsets, and a 12 mm Gaussian filter was applied. Segmentations were performed by placing spherical volumes matching the physical sphere volumes using the CT images and extracting the mean counts. The mean background count was estimated by placing a cylindrical volume with a 20-mm radius and 18-mm height in the region between the spheres.

We used contrast to illustrate visualization. Contrast was calculated with

$$contrast = \frac{(C_{sphere} - C_{background})}{C_{sphere}}$$

where C_{sphere} is the mean counts in a spherical region of interest, and $C_{background}$ is the mean background count. Contrast was plotted as a colormap in MATLAB (version R2023b) by displaying a two-dimensional view of an interpolated a three-dimensional mesh of sphere volumes, sphere activity concentrations, and contrast. In Figure 6 below, the lines show the actual activity concentrations and volumes of the spheres used in the interpolation.

The patient structures were added to the plot by converting the SUVmean value from the PSMA-PET (given in Tables 3 in the publication and Supplemental file 2) to activity concentration with ^{212}Pb, $A_{conc}(^{212}Pb)$, according to

$$A_{conc}(^{212}Pb) = \text{SUVmean} \times \frac{A_{inj,dec}}{BW}$$

where BW is the patient body weight, and $A_{inj,dec}$ is the decay corrected injected activity of ^{212}Pb. The volumes of the tumors and parotid were estimated by thresholds on the PET set with the CT as a guide. For patient ID01 the acquisition time per bed position was 20 minutes, rather than 30 minutes, and therefore the estimate for activity concentration was scaled by 0.667.

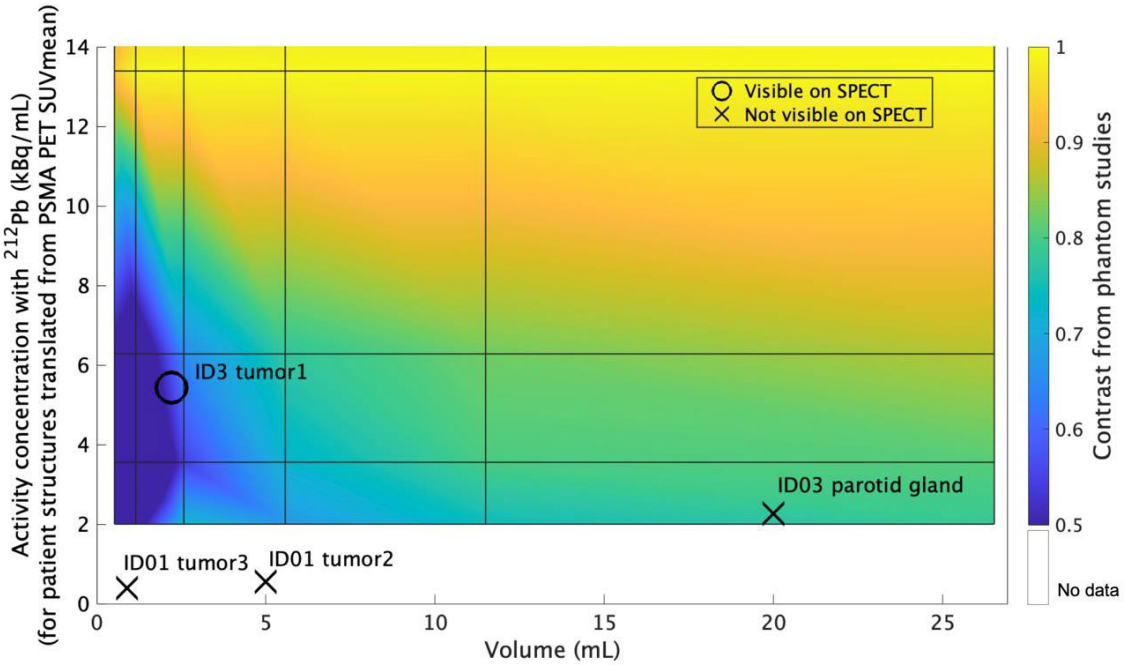

FIGURE 6: The illustration included as Figure 4 in the publication, with additional lines which show the activity concentrations and volumes from which the contrast map was interpolated. Higher activity concentrations were also included in the interpolation, but as not relevant for the ^{212}Pb microdose used in the trial are absent from the figure.